Statistical Analyses of Wind Field Obtained from Short Interval VISSR Observations

Isao Takano* and Kazuo Saito*

Abstract

Low level wind vectors in high spatial resolution were derived by auto-tracking technique from short-time interval VISSR observations over the Japan Sea in NOV. 1984. Statistical features of the wind field were examined. Auto correlation analysis showed strong anisotropy of both u and v component of the wind. Random errors of the derived wind data were estimated by means of structure functions and showed some dependency on two auto-tracking parameters, i.e., template sizes and scan-time intervals. Derived vector number decreased remarkably as scan-time interval increased.

1. Introduction

Cloud motion observations have been performed from GMS-series VISSR imagery since 1978 when GMS began its operation. Automated cloud tracking procedure has enabled to derive a large number of low-level cloud vectors rapidly from 30 minutes interval images.

Utility of short-time interval imagery has been discussed in some articles. Johnson et al. (1980) has pointed out that number of trackable clouds diminished as the scan-time interval increased.

Maddox et al. (1979) examined the statistical structure of mesoscale satellite winds with 5 minutes interval images using structure functions and auto correlations and depicted anisotropy of the wind field. They estimated a random error to be less than 1.75 m/s.

Wylie et al. (1981) calculated spatial auto correlations of zonal and meridional component of satellite winds over the Indian Ocean for both longitudinal and transverse directions.

Authors' attempt is to apply automated cloud tracking procedure to short-time interval imagery and to examine dependence of data on two tracking parameters, i.e. scan-time intervals and tracking template sizes. Anisotropy of the wind field was examined by use of two-dimensional auto correlations and radnom errors were estimated from structure functions.

2. Data

a. Cloud tracking

Short-time interval GMS-3 VISSR observations were made around Japan from 0433 GMT to 0506 GMT on 27 NOV. 1984 and 7 images of about 6 minutes interval were obtained sequentially.

Wind vectors were derived from two of seven images in the Japan Sea area of 44°–34°N, 130°–145°E by automatic cloud tracking technique of the Meteorological Satellite Center which uses cross correlation method.

In the procedure a template containing the low-level target cloud, whose center is located at the grid point, was extracted from the original visible image. Cross correlation calcula-

*Numerical Prediction Division, Japan Meteorological Agency.

tions were performed between the template and the searching area of the following image, which gives the movement of the cloud. Details of the procedure have been described by Hamada (1979).

Several vector sets of different tracking parameters were obtained for comparison. The template size, the scan-time interval and other tracking parameters used in the examination are compared with those used routinely (Table 1).

Table 1. Initial parameters adopted in cloud wind estimation

PARAMETERS	ROUTINE	EXAMINED
prepared images	A B C	B C
image scan-time intervals (min.)	30	6, 11, 17, 22, 28
number of matching steps	(2, 2)	2
sampling rate for coarse matching (pixel, line)	(4. 3)	(2, 2)
target selection area	50°N—50°S 90°E—170°W	44°N—34°N 130°E—145°E
lat. and long. target selection intervals	(1.0, 1.0)	(.25, .25)
target selection number	600	1200
template sizes (pixel, line)	(32, 32)	(8, 8) (16, 16) (32, 32)
upper boundary pressure level (mb)	700	550

Fig. 1 shows the VISSR visible image for 0300 GMT 27 NOV. With a strong outflow of cold air from Siberia low-level cumuli occurred over the Japan Sea. Those cumuli have altitude of 2–3 km and diameter of about 10 km.

Horizontal resolution of the VISSR visible image around this region is 1.0 km for pixel, 2.1 km for line.

b. Wind vector features

Fig. 2 shows the result of cloud tracking with template of 16 pixels x 16 lines and time interval of 11 min. Wind vectors were derived at almost all points where low-level cumuli exist, which implys that satellite imagery may offer informations for motions of small-scale disturbances. In this case, however, there can be seen little variation of wind with space and no prominent small-scale feature is found. Almost all clouds moved SE-ward with speed of 10 m/s.

Some wind vectors near the coast of the Continent are inconsistent with adjacent vectors. These vectors were found to be erroneous by cloud movement check on the Image Processing Console of MSC and were excluded from the statistical analyses, because our present concern is about random errors of the data.

c. Number of wind vectors

Results obtained from the automatic tracking procedure are internally checked in terms of maximum correlation value, difference between the first maximum correlation value and the second maximum one, difference of cloud top heights calculated from two images etc., which are affected by tracking parameters. Thus number of extracted vectors is dependent on these parameters. Roles of template size and scan-time interval were examined by changing their values. Numbers of extracted wind vectors in cases of template of 8 pixels

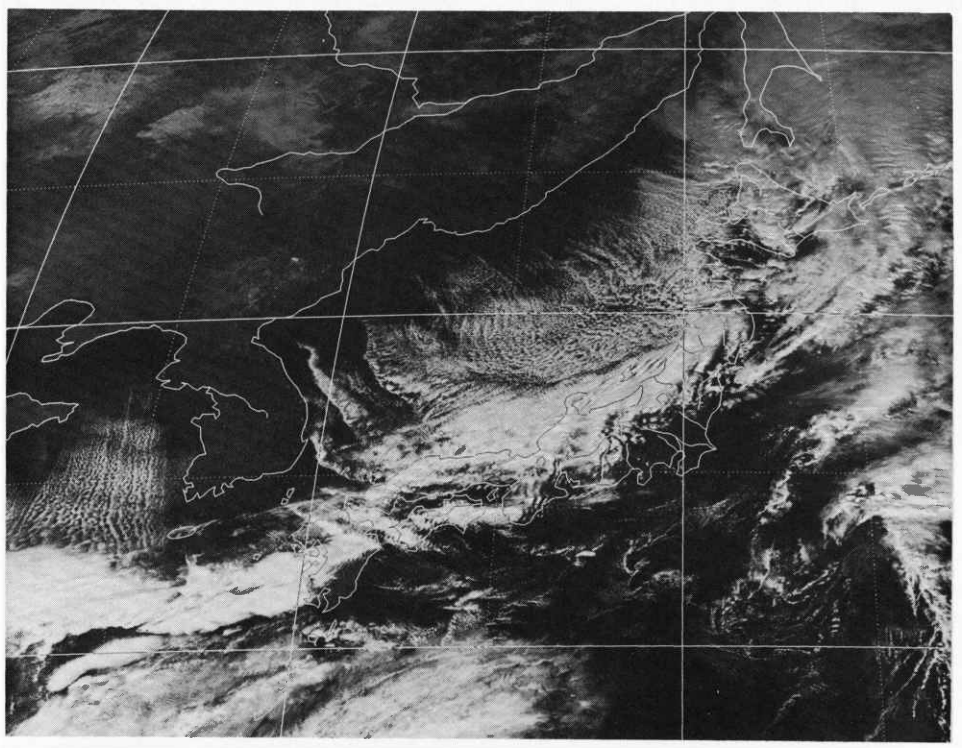

Fig. 1. VISSR visible image at 03GMT NOV. 27.

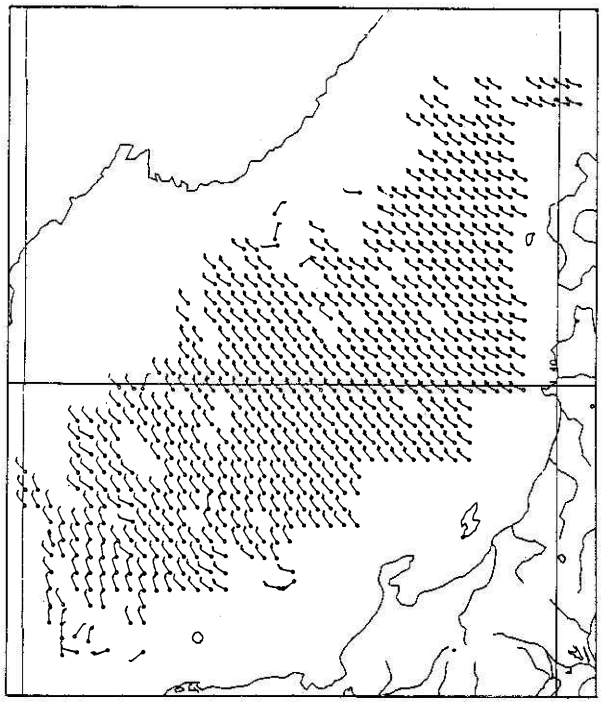

Fig. 2. Satellite low-level winds on the Japan Sea in the case of template of 16 x 16 and scan-time interval of 11 min.

x 8 lines, 16 x 16 and 32 x 32 and scan-time interval of 6 min., 11, 17, 22 and 28 min. are compared in Fig. 3.

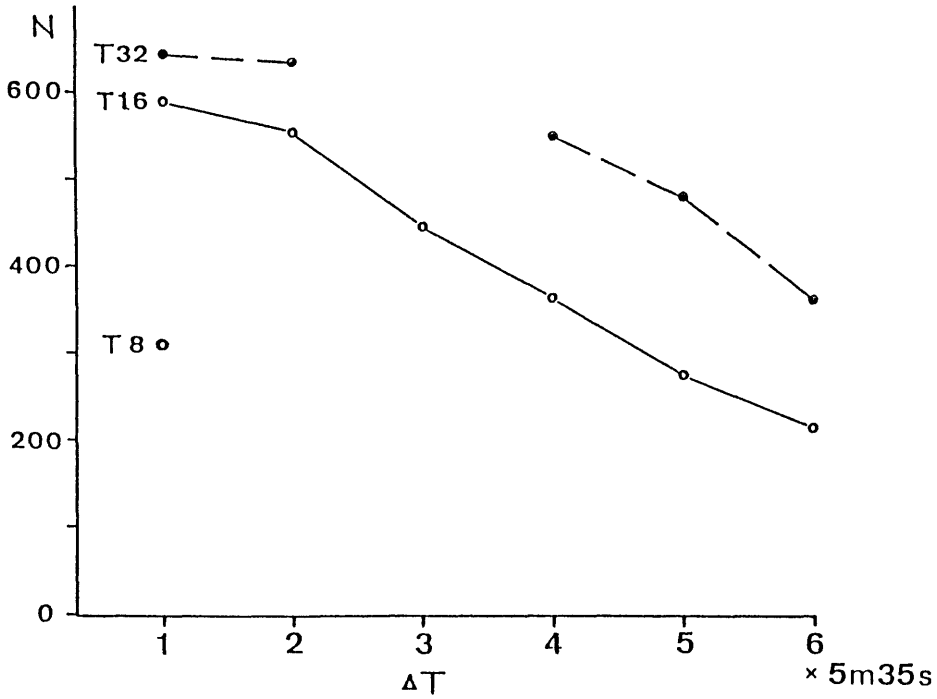

Fig. 3. Extracted vector numbers for templates of 8 x 8, 16 x 16 and 32 x 32 and scan-time intervals of 6, 11, 17, 22, 28 min.

Tracked cumulus changes its shape and size with time which makes accurate tracking of a cumulus difficult. As a result, number of extracted vector decreased as scan-time interval increased, as in Fig. 3. This trend is outstanding in cases of scan-time interval longer than 17 min.

On the other hand, a smaller template resulted in less wind data. A case of template of 8 pixels x 8 lines offered only half as much as the cases of 16 pixels x 16 lines or 32 x 32. A template of 8 x 8 is about the size of a typical cloud cell which may not be large enough for precise calculation of movement of a whole cell.

From above examination it is inferred that it is important to choose proper tracking parameters in order to obtain sufficient data to analyze small scale features which generally have short lifetimes. In order to obtain high-resolution wind vectors, selecting a comparatively large template is advantageous, but a large template apparently doesn't represent movement of small-scale features. Thus in this case scan-time interval of less than 15 min. and a template slightly larger than the target, about 20 km x 20 km could be recommended. Selecting short scan-time interval is also important from a observational point of view, because long scan-time interval tends to obscure minute structure of the phenomena.

3. Statistical analysis

From these observation data several statis-

tical parameters were evaluated for u and v component of wind data sets. These are ensemble means ($\overline{A}$), standard deviations (σ_A), two-dimensional auto correlation functions (C_A) which are functions of latitudinal distance and longitudinal distance between two points and two-dimensional structure functions (D_A).

$$\overline{A}=\frac{1}{N}\sum_{i,j}A(\varphi_i,\ \lambda_j)$$

$$\sigma_A=\sqrt{\frac{1}{N}\sum_{i,j}(A(\varphi_i,\ \lambda_j)-\overline{A})^2}$$

$$C_A(\Delta\varphi,\ \Delta\lambda)$$

$$=\frac{\sum_{i,j}A'(\varphi_i,\ \lambda_j)\circ A'(\varphi_i+\Delta\varphi,\ \lambda_j+\Delta\lambda)}{\sqrt{\sum_{i,j}A'(\varphi_i,\ \lambda_j)^2}\cdot\sqrt{\sum_{i,j}A'(\varphi_i+\Delta\varphi,\ \lambda_j+\Delta\lambda)^2}}$$

$$D_A(\Delta\varphi,\ \Delta\lambda)$$

$$=\frac{1}{M}\Sigma(A(\varphi_i+\Delta\varphi,\ \lambda_j+\Delta\lambda)-A(\varphi_i,\ \lambda_j))^2$$

where N is the data number, M is the number of data pairs, A' is the deviation of wind from ensemble means, φ_i, λ_j are the latitude and the longitude of wind location and $\Delta\varphi$, $\Delta\lambda$ are the latitudinal and longitudinal distances between two points.

Auto correlation functions were normalized by the value adjacent to the origin. By this normalization procedure, auto correlation functions are free from random errors which are assumed to be independent of space. For variables varying smoothly with space auto correlation funcitons tend to decrease with distance from unit at origin.

Generally structure functions tend to increase with distance. As shown below, structure functions approach twice the square of random errors as the distance between two points approaches zero if the random errors are not spatially correlated.

Raw observation data contain spatial distribution of wind and observation errors, and can be expressed as

$$u = \hat{u} + u^*$$

where u is the observed wind, $\hat{u}$ is the spatial distribution of wind and u* is the observation errors. Observation errors are assumed to be random and to have no spatial correlation, i.e.,

$$C^*(\Delta x) = 1 \quad \text{where } \Delta x = 0$$
$$= 0 \quad \text{where } \Delta x > 0$$

where Δx is the distance between two points.

Then the structure function

$$D(\Delta x)=\frac{1}{N}\Sigma(u(x+\Delta x)-u(x))^2$$

$$=\hat{D}(\Delta x)+D^*(\Delta x)$$

$$D^*(\Delta x)=\frac{1}{N}\Sigma u^*(x+\Delta x)^2+\frac{1}{N}\Sigma u^*(x)^2$$

$$-\frac{2}{N}\Sigma u^*(x+\Delta x)\cdot u^*(x)$$

as u*(x) is assumed to have no spatial correlation

$$D^*(\Delta x)=2\delta^{*2} \quad \text{where } \delta=\frac{1}{N}\Sigma u^{*2}$$

and as $\Delta x\to 0$, $\hat{D}(\Delta x)\to 0$

$$\therefore\ \Delta x\to 0, \quad D(\Delta x)\to 2\delta^{*2}$$

Observation errors of random character were thus estimated from structure functions.

a. Random error estimation

Estimation of random errors were accomplished in conjunction with standard deviations of raw observation data and are shown in Fig. 4 for template of 16 x 16, 32 x 32 and scan-time interval of 6–28 min.

Standard deviations of u component are about 5.5 m/s and have little dependence on

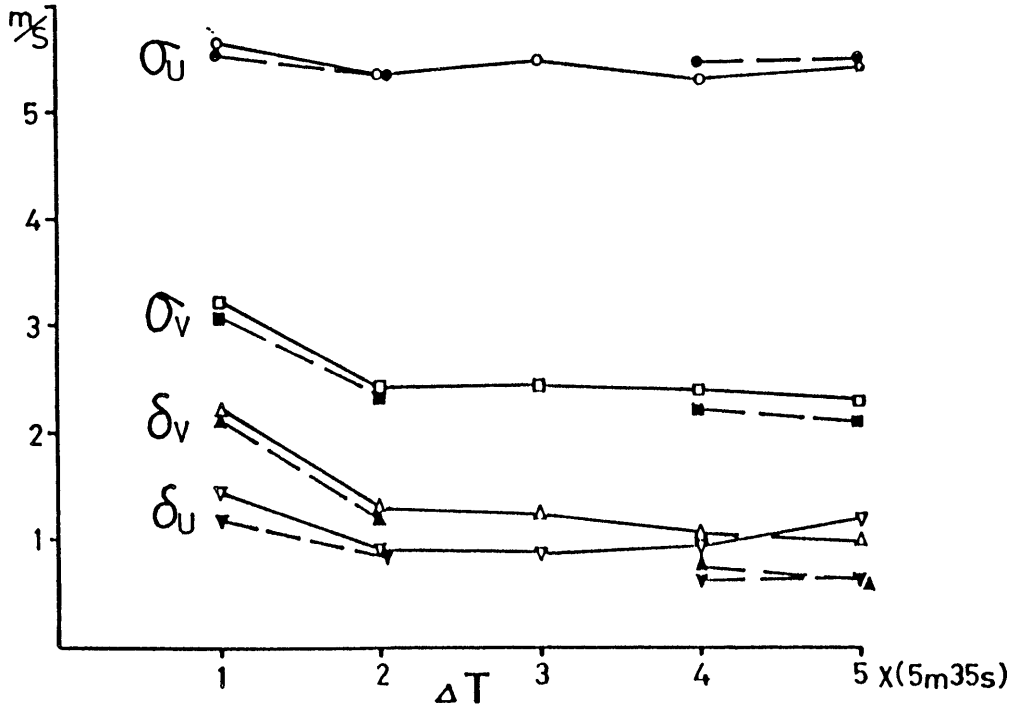

Fig. 4. Standard deviations of the observed winds (σ, m/s) and random errors estimated from structure functions (δ, m/s). The solid lines are for template of 16 x 16 and the dashed lines are for template of 32 x 32.

both scan-time intervals and template sizes. Standard deviations of v component are about half as much as those of u component and have approximately equal values except in the cases of scan-time interval of 6 min. where standard deviations are larger than other cases.

In cases of template of 16 x 16, random errors of u component are about 1 m/s and are slightly larger in the cases of time interval of 6 min. and 28 min. Random errors of v component are 40–50% larger than those of u component in the cases of short time intervals. They tend to decrease with time interval. Random error at time interval of 6 min is exceptionally large, exceeding 2 m/s.

In cases of template of 32 x 32, errors are smaller than those of template of 16 x 16, especially in the cases of longer time intervals.

Large random errors of time interval of 6 min. can be explained by VISSR image granularity, which was discussed by Hamada (1983). The fact that random errors of v component are generally larger than those of u component is also attributable to image granularity because one pixel gap which approximately determines the accuracy of u components is about half as much as one line gap which corresponds to v component.

These image granularity errors diminish as scan-time interval increases. Random errors of template of 16 x 16, however, don't decrease as expected in the longer scan-time intervals. It is presumably due to augmentation of tracking error owing to deformation of target clouds.

Random errors discussed so far are comparable to random errors of 1.5 m/s estimated

by Maddox et al. (1979) for GOES satellite winds.

The ratio of δv to σv is about 50%, which indicates that considerable part of observation data is contaminated by random errors, while the ratio of δu to σu is much smaller.

b. Spatial correlation function

In order to examine spatial characteristics of wind field, two dimensional auto correlation functions were calculated for u and v component of the wind. Some examples of template of 16 x 16, 32 x 32 and scan-time interval of 11, 22 min. are shown in Fig. 5. Note that Fig. 5 shows only a half of the field where longi-

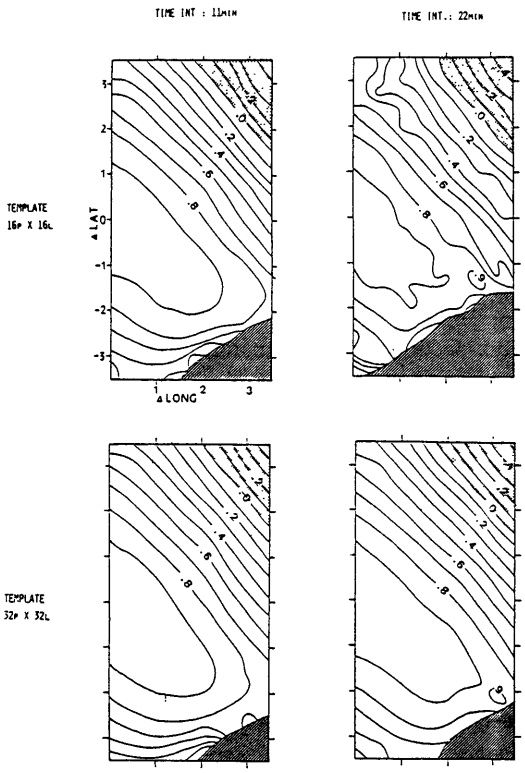

Fig. 5a. Two-dimensional auto correlation coefficient in cases of template of 16 x 16 (upper), 32 x 32 (lower) and scan-time interval of 11 min. (left), 22 min. (right) for u component of the wind filed.

tudinal distance is positive because the auto correlation function is symmetric about its

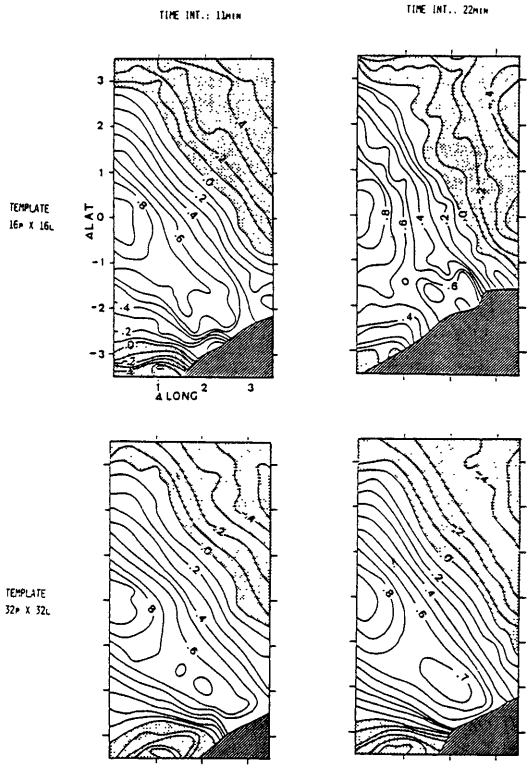

Fig. 5b. Two-dimensional auto correlation coefficient for v component.

origin. Auto correlations were calculated at each 0.25 degree interval points for latitudinal and longitudinal distance of 3.5 degrees except in hatched area in Fig. 5 where data pairs were less than 30. Areas of negative auto correlations are marked with shading. Fig. 5 shows that for u and v component wind field is remarkably anisotropic with high auto correlation area elongated along NW–SE, which is oriented slightly in the right-hand direction of the mean wind. The auto correlation function of the u compoment is remarkable for its vast area of high value 0.9 which extends more than 200 km, while that of the v component decreases more rapidly.

Integration of an auto correlation function between the origin and the point where it becomes zero can be considered as the measure

a)

TEMPLATE (P×L) \ T. INT. (min)	11	22
16×16	215.9	197.6
32×32	223.9	214.7

b)

TEMPLATE (P×L) \ T. INT. (min)	11	22
16×16	107.2	108.3
32×32	110.4	100.0

Table 2. Characteristic lengths of the wind field obtained by integration of two-dimensional auto correlation coefficients along the cross-wind direction for positive-value area (km).
a) for u component
b) for v component

of horizontal scale representing the motion. The integrations performed in the cross-wind direction are compared in Table 2. The integrated lengths of u component are about 200 km, and are about twice of those of v component. Larger templates generally bring slightly longer characteristic lengths. On the other hand, longer scan-time intervals don't present longer characteristic lengths.

It may be concluded that spatial variations of wind field are slightly smoothed by choosing a larger template, while they aren't affected by scan-time intervals.

4. Summary and Discussions

Automatic cloud tracking procedure was applied to short-time interval VISSR images when winter cellular cumuli appeared on the Japan Sea and produced dense low-level wind data. Comparison of cases with various tracking parameters showed that in order to obtain high-density data is requires short time intervals and tracking templates of a size larger than the target clouds.

Random errors of derived wind data were estimated from the structure functions to be 1–2 m/s. Those of cases of scan-time interval of 6 min. were larger than other cases, which is due to granularity of the imagery. In cases of short scan-time intervals random errors of v component are larter than those of u component. Estimated random errors are comparable to those estimated by Maddox et al. (1979) for GOES imagery.

Observation errors were estimated under the assumption that they have no spatial correlation, however, this assumption needs further investigation for its validity.

It was made clear that for acquistiion of accurate and high-density meso-scale wind data, a tracking template of 16 pixel × 16 line and a scan-time interval of 11 min. were most suitable in this case study.

Two-dimensional auto correlation analysis of the wind field has exhibited that it has significant anisotropy with high auto correlation occurring approximately along the mean wind direction and that u component of the wind was more spatially correlated than v component with a characteristic length of 200 km, compared to 100 km. These values are of the same order with one-dimensional auto correlations calculated by Maddox et al. (1979).

The examined wind field involved no conspicuous small-scale features, thus two-dimensional auto correlations showed little dependence on tracking parameters.

Acknowledgements

The authors appreciated the comments of T. Hamada, T. Oshima and A. Segami on the statistical analysis of satellite winds. We also would like to thank the staff of MSC for their willing assistance.

References

Maddox, R.A. and T.H. Vonder Haar, 1979: Covariance analyses of satellite-derived mesoscale fields. J. appl. Meteor., 18, 1327–1334.

Wylie, D.P. and B.B. Hinton, 1981: Some statistical characteristics of cloud motion winds measured over the Indian Ocean during the summer monsoon. Mon. Wea. Rev., 109, 1810–1812.

Johnson, G.L. and D. Suchman, 1980: Intercomparisons of SMS wind sets: A study using rapid-scan imagery. Mon. Wea. Rev., 108, 1672–1688.

Hamada, T., 1979: Cloud Wind Estimation System Summary of GMS System. Meteorological Satellite Center Technical Note (Special Issue II-2), 15–42.

Hamada, T., 1983: On the Optimal Time-interval of Satellite Image Acquision for Operational Cloud Motion Wind Derivation. Meteorological Satellite Center Technical Note, No. 7, 79–87.

短時間間隔 VISSR 観測から求めた風の場の統計的解析

高野　功・斎藤和雄

気象庁予報部数値予報課

1984年11月に得られたGMS−3のマルチセグメント画像から季節風吹き出し時の日本海の下層風ベクトルを自動雲追跡法により高密度に求めた。風ベクトル算出時の画像切り出しサイズ（テンプレート）と撮像時間間隔をいくつか選び結果を比較した。

得られた風ベクトルの個数は撮像間隔が長くなると共に減少した。また雲のセルと同程度の大きさのテンプレートではより大きなテンプレートの場合と比較して個数は半減した。

構造関数から求めたランダム誤差はV成分がU成分より大きく，最短撮像間隔（6分）の場合がU，V成分共他の場合より大きかった。これらは画像の量子化誤差の影響と考えられる。撮像間隔が10分以上の場合，ランダム誤差のU，V成分の差は小さく，誤差は1m／s前後であった。

風ベクトルの個数とランダム誤差の考察から，小スケールの現象を解析しようとするには今回の事例では，テンプレートが16ピクセルX16ライン，撮像間隔が11分の場合が最も適していることがわかった。

次に2次元の相関係数を用い下層風の空間特性を調べたところ，U，V成分とも強い異方性を示し，両者の高い相関の軸は平均風の方向とほぼ一致した。またV成分がU成分より原点から離れるにつれ急速に相関が小さくなった。相関係数の風計算パラメータへの依存性ははっきり現われなかった。